TDPAC studies on the recovery of Ag plastically deformed at room temperature

1989 J. Phys.: Condens. Matter 1 7521

(http://iopscience.iop.org/0953-8984/1/41/002)

J. Phys.: Condens. Matter 1 (1989) 7521–7528. Printed in the UK

TDPAC studies on the recovery of Ag plastically deformed at room temperature

B Wodniecka, M Marszałek and P Wodniecki
Institute of Nuclear Physics, Radzikowskiego 152, 31-342 Cracow, Poland

Received 20 October 1988

Abstract. The recovery of polycrystalline silver rolled at room temperature to different degrees of deformation (33, 48, 73 and 95%) was investigated by means of the TDPAC technique with a ^{111}Cd probe. The dependence of quadrupole interaction parameters, extracted from time spectra, on the degree of deformation and annealing temperature was studied. At temperatures in the range 350–425 K the recovery stage occurs which is indicated by the decrease of quadrupole interaction. For lower degrees of deformation also a small fraction (~2%) of sharp quadrupole frequency of 38(1) MHz was detected after annealing at temperatures 300–375 K, associated with vacancy complexes trapped on probe atoms.

1. Introduction

The time-dependent perturbed angular correlation method (TDPAC) is a very useful tool for the study of static and dynamic properties of defects. Like NMR and the Mössbauer effect, PAC is a microscopic probe technique which can detect the coupling between nuclear moments and extra-nuclear fields. In the case of the PAC method the hyperfine interaction most relevant to defect studies is the electric quadrupole interaction. In FCC cubic metals defects destroy the perfect cubic lattice symmetry inducing an electric field gradient (EFG) at the site of the probe atom. Unlike neutron scattering, resistivity, channelling, x-ray and positron lifetime techniques, which yield a signal that is related to the total of all defects, PAC provides for each defect a unique flag, i.e. the quadrupole interaction frequency, by which it can be distinguished from others. One can clearly resolve different probe–defect configurations which are formed as a result of defect migration and trapping and hence obtain a valuable microscopic picture of defect phenomena in damaged materials.

The study of elementary point defects has been the object of extensive experimental and theoretical works. The investigation of larger defects is of interest to technologists who are concerned with work-hardened metals. In this case the cold working does produce defects. The damage induced by plastic deformation consists mainly of a network of dislocations. But it is generally known that, when deforming a metal sample, one introduces also a certain amount of vacancies and vacancy complexes. Since the first application of PAC [1, 2] to study defects in deformed metals, a number of results have been obtained [3–12]. In cold worked metals mainly the trapping of point defects and vacancy clusters on probe atoms was observed. No trapping of dislocations was found. Only in considerably deformed Al^{57}Cu studied with Mössbauer spectroscopy [11] has

0953-8984/89/417521 + 08 $02.50

the defect line related to probe atoms located in regions of densely packed dislocations been observed. The understanding of the defect structure obtained in these experiments and the defect behaviour occurring during thermal annealing of the cold worked samples is far from being complete. This might be caused by the lack of information about the concentration and distribution of different types of defects present in the sample after the damage procedure.

In most experiments with cold worked metals the deformation was performed at liquid nitrogen temperature; that means far below the recovery stages describing the behaviour of point defects. During room temperature deformation point defect-like species are instantaneously annealed and one can expect to observe in this case only the more extended defects and dislocations.

In this work the TDPAC method was used to investigate the recovery of polycrystalline silver plastically deformed at room temperature. The stage V recovery was observed by measuring the annealing-induced changes of low-frequency distribution which are believed to be connected with dislocation density. Also the small fraction of probes interacting with sharp quadrupole frequency due to vacancy complexes (probably planar faulted loops) was observed. No trapping of dislocations on probe nuclei was found.

2. Experimental procedure

Polycrystalline Ag foils of 4N purity and 50 μm thick were irradiated with the 28 MeV α-beam of the Cracow cyclotron to produce ^{111}In nuclei via the ^{109}Ag $(\alpha, 2n)^{111}$In nuclear reaction. Foils containing ^{111}In activity were then annealed for two hours at 600 K in a vacuum in order to obtain damage-free **Ag**^{111}In samples. The unperturbed TDPAC patterns obtained after annealing indicated the undisturbed cubic surrounding of the ^{111}In probe atoms. Samples were then plastically deformed at room temperature by rolling. The area extension gave values for the degree of deformation ε equal to 33(10), 48(10), 73(10) and 95(10)%, respectively. All samples were subjected to isochronal annealing sequences. Annealings were performed in vacuum in the temperature range 300–600 K. The annealing time was 30 min at each step. PAC measurements were done directly after rolling and after each annealing step.

For the TDPAC measurements a standard slow–fast coincidence system with four (2 in × 2 in) NaI(Tl) detectors was used. The time resolution of the system was about 3.5 ns FWHM if gated on the 171–245 keV γ–γ cascade of ^{111}In. The source–detector distance was 4 cm resulting in the effective anisotropy coefficient $A_2^{\text{eff}} = -0.127$. From four coincidence spectra recorded simultaneously during each measurement, the following ratio was calculated [13]:

$$R(t) = \frac{\{C_{13}(t,\pi)C_{24}(t,\pi)\}^{1/2} - \{C_{14}(t,\pi/2)C_{23}(t,\pi/2)\}^{1/2}}{\frac{1}{2}\{c_{13}(t,\pi)C_{24}(t,\pi)\}^{1/2} + \{C_{14}(t,\pi/2)C_{23}(t,\pi/2)\}^{1/2}} = A_2^{\text{eff}} G_2(t). \tag{1}$$

Here, $C_{ij}(t, \theta)$ is the background-corrected coincidence rate for detector i and detector j; θ is the angle π or $\pi/2$ between these detectors.

The perturbation factor $G_2(t)$ which modulates the lifetime curve of the 247 keV nuclear level of ^{111}Cd obtained from (1) was least-squares fitted by an expression of the form

$$G_2(t) = \sum_i f^{(i)} G_2^{(i)}(t) \tag{2}$$

where $f^{(i)}$ are relative fractions of probe nuclei and $G_2^{(i)}(t)$ are functions of quadrupole

interaction parameters: the quadrupole frequency $\nu_Q^{(i)}$, the asymmetry parameter $\eta^{(i)}$ and the width of quadrupole frequency distribution $\delta^{(i)}$.

3. Results and discussion

Two different kinds of hyperfine interaction can be found in most damaged FCC metals, depending on the relative distance between the defect and the probe atom. This is seen in the TDPAC measurements as two distinct frequency patterns: a low-frequency distribution due to defects situated at various distances from the probe nuclei and a high sharp frequency generated by defects located in the nearest neighbourhood of the probe.

In FCC metals deformed at room temperature, in practice, only the dislocations and extended vacancy clusters are stable. The vacancies and other point defects, because of

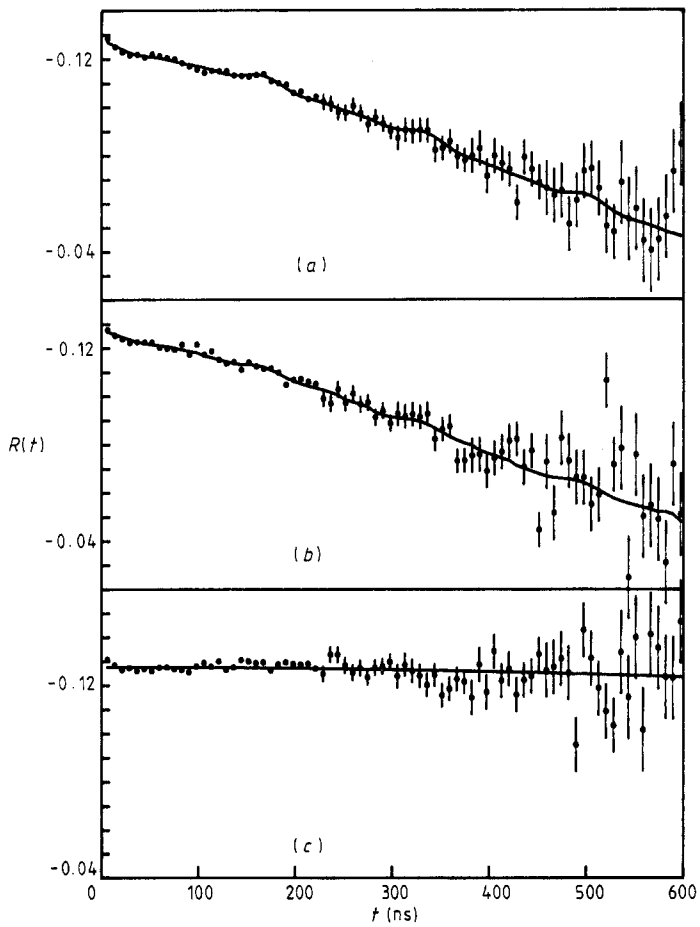

Figure 1. PAC spectra of ^{111}Cd in a polycrystalline Ag sample rolled to 50% deformation taken at room temperature after 30 min annealings at temperatures T_{ann} = 330 (*a*), 375 (*b*) and 425 K (*c*). The full curves represent the results of least-squares fits to the data according to expression (3).

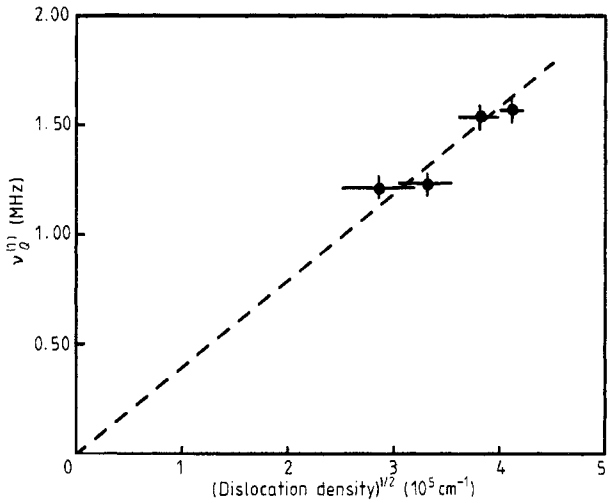

Figure 2. Quadrupole frequency $\nu_Q^{(1)}$ measured in rolled Ag samples at room temperature as a function of a dislocation density deduced from the degree of deformation, based on the results reported in [25, 26].

their low activation energy of motion, exhibit considerable mobility and consequently became annihilated at once during the deformation.

Figure 1 shows some examples of the PAC results of an annealing sequence for ^{111}In-doped deformed Ag specimens. The full curves represent the results of least-squares fits to the experimental data according to

$$A_2^{\text{eff}} G_2(t) = A_2^{\text{eff}} \left[(1-f) \sum_n s_{2n} \cos\left(n \frac{3\pi}{10} \nu_Q^{(1)} t \right) \exp(-n\delta^{(1)} t) + f \sum_n s_{2n} \cos\left(n \frac{3\pi}{10} \nu_Q^{(2)} t \right) \right]. \tag{3}$$

The first term in brackets stands for a predominant fraction (>98%) of the probe nuclei which interact with axially symmetric EFG described by the Lorentzian distribution of quadrupole frequencies with width $\delta^{(1)}$ around the centroid $\nu_Q^{(1)}$. This EFG distribution may be assigned to dislocations introduced during rolling. The width $\delta^{(1)}$ of the distribution resulting from the fit was about 30% of $\nu_Q^{(1)}$ and decreased with increasing annealing temperature. The $\nu_Q^{(1)}$ values extracted from the recorded spectra are shown to depend on the deformation degree of the sample ε (as illustrated in figure 2) and annealing temperature T_{ann} (figure 3).

The second term in (3) represents a small (~2%) fraction f of the probes interacting with the unique axially symmetric EFG. These In atoms are decorated with identical defects of a unique configuration. The quadrupole frequency $\nu_Q^{(2)} = 38(1)$ MHz was observed only in 33 and 48% deformed Ag samples. The annealing behaviour of this component is shown in figure 4. After annealing at 400 K this fraction vanishes. We propose to interpret this component as due to vacancy clusters, probably faulted vacancy loops. This fraction was not found in more deformed samples ($\varepsilon = 73$ and 95%). A possible explanation is the competition between vacancy cluster formation and vacancy annihilation on dislocations during cold working. A few percentage fractions of similar

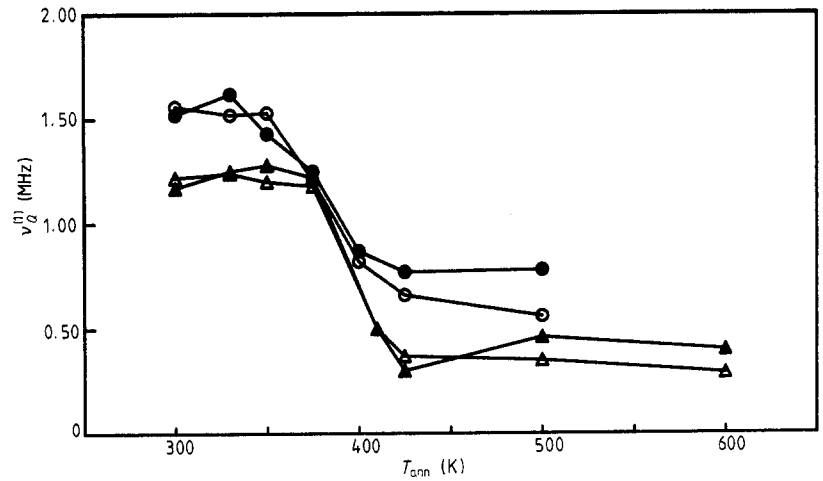

Figure 3. Quadrupole frequency $\nu_Q^{(1)}$ measured in Ag rolled at room temperature to different degrees of deformation (ε = (△) 33, (▲) 48, (○) 73, (●) 95%) after 30 min annealings at temperatures T_{ann}.

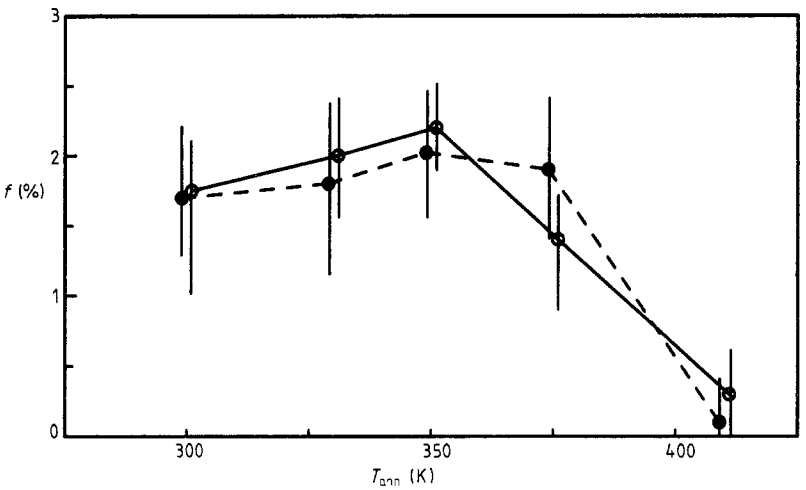

Figure 4. Fraction f of quadrupole frequency $\nu_Q^{(2)}$ = 38(1) MHz observed after annealings at temperatures T_{ann} in Ag rolled to the deformations ε = (○) 33 and (●) 48%.

frequency, 36(2) MHz, but higher stability, were observed in silver by Deicher [14] after electron irradiation and by Thomé [15] after implantation. In our earlier experiment [16] the 38 MHz component, stable up to 420 K, was detected in proton-irradiated silver. The different thermal stability of vacancy loops trapped at ^{111}In, most probably connected with cluster dimensions, was also observed in Cu [17], Au [18, 19] and Ni [20].

Dislocations produce in their surrounding a local strain field leading to the local EFG which would cause a quadrupole interaction. At sufficiently large distances from the defect site the induced strains and stresses can be described by linear elasticity theory

and the EFG can be calculated if the gradient elastic constants are known. In a metal a redistribution of conduction electron charge density occurs near a dislocation, analogous to the behaviour around point defects. However, an estimate shows that, up to very high dislocation density of the order of 10^{11} cm^{-2}, the influence of the conduction electrons on the total dislocation-induced quadrupole perturbation remains below 1% [21]. Treating the host lattice as an isotropic homogeneous continuum and supposing a random distribution of dislocations one can derive the distribution function of the quadrupole frequencies resulting from the quadrupole interaction of probe atoms with EFG produced by dislocations.

It was shown [22] that the mean EFG at a distance r from the dislocation line can be expressed as

$$V_{zz}(r) \simeq \frac{Gb}{2\pi} S_{44} r^{-1} = A_\sigma r^{-1} \tag{4}$$

where G is the shear modulus, b the modulus of the Burgers vector and S_{44} the gradient elastic constant.

Randomly distributed dislocations of density c result in the distribution of the mean EFG of the form [23, 24]:

$$p(V_{zz})\,\mathrm{d}V_{zz} = \pi A_\sigma^2 |V_{zz}|^{-3} c \exp(-\pi c (A_\sigma / V_{zz})^2)\,\mathrm{d}V_{zz}. \tag{5}$$

Since the quadrupole frequency ν_Q is associated with the electric field gradient V_{zz} according to

$$\nu_Q = eQV_{zz}/h \tag{6}$$

(where eQ is the quadrupole moment, h the Planck constant), the corresponding expression for the distribution of strain-induced quadrupole frequencies is

$$p(\nu_Q)\,\mathrm{d}\nu_Q = \pi c A_\sigma^2 |\nu_Q|^{-3} \exp(-\pi c A_\sigma^2 \nu_Q^{-2})\,\mathrm{d}\nu_Q. \tag{7}$$

Introducing the normalised frequency $s = \nu_Q/(A_\sigma \sqrt{\pi c})$ leads to the normalised form:

$$p(s)\,\mathrm{d}s = |s|^{-3} \exp(-s^{-2})\,\mathrm{d}s. \tag{8}$$

Thus the width of the distribution as well as the mean value of the quadrupole frequencies caused by dislocation-induced EFG are shown to be proportional to the square root of the dislocation density c, in contrast to the case of randomly distributed point defects, where the quadrupole interaction is proportional to the defect density [23]. The measured $\nu_Q^{(1)}$ mean values of the quadrupole frequency distributions attributed to quadrupole interaction of probes with EFG produced by dislocations (equation (3)) are presented in figure 2 as functions of $\sqrt{c}$. Each $\nu_Q^{(1)}$ in figure 2 for a given deformation is taken as the average value of the data from the initial flat region of the corresponding annealing curve $\nu_Q^{(1)}(T_{\mathrm{ann}})$ (see figure 3). Dislocation density values c were deduced from the degree of deformation ε obtained from the interpolation of the results reported in [25, 26]. The linear dependence of $\nu_Q^{(1)}$ on the square root of the dislocation density is observed; however the uncertainty in the determination of dislocation density c must be considered.

Fairly extensive studies on the recovery of cold worked FCC metals have been performed by electrical resistivity measurements [27, 28]. The recovery stage V attributed to the rearrangement and annihilation of dislocations and hence to recrystallisation would be expected to show activation enthalpy similar to that of self-diffusion. The latter value is for Ag 1.91(1) eV [29]. The recovery experiments have yielded smaller

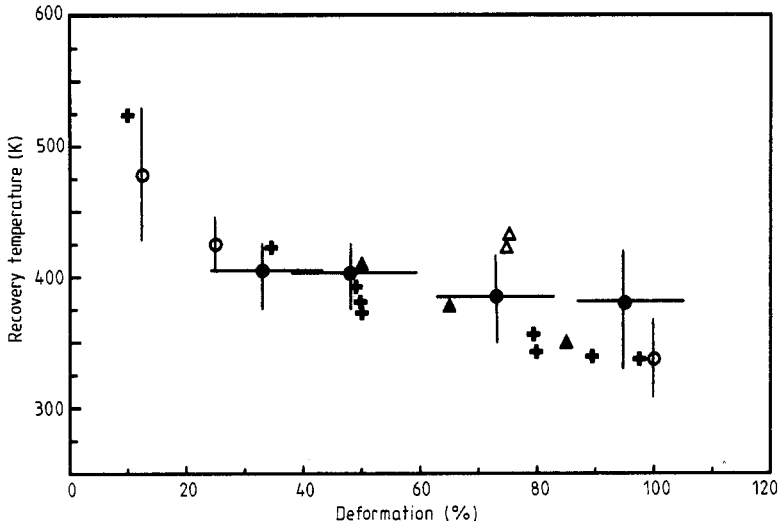

Figure 5. Recovery temperatures of cold worked silver as a function of the degree of deformation. The data are results of hardness measurements [26 (△), 35 (+)], residual resistivity experiments [26, 30 (▲), 35], positron lifetime studies [36 (○)] and this work (●).

values. The reported activation temperatures and energies associated with recovery stage V in silver are spread between $T = 340$–670 K and $E = 0.85$–1.92 eV [30–34]. The lower values of the activation energy could be connected with cross slipping (rearrangement) of dislocations, while the higher values could be connected with annihilation of dislocations and recrystallisation. This is in agreement with calorimetry and TEM measurements in cold worked silver [25].

The stage V recovery temperature depends on the degree of deformation as shown in hardness [35] and residual resistivity experiments [30, 35]. With very large internal stresses the thermodynamic instability of the internal stresses occurs at lower temperatures. The recrystallisation is also influenced considerably by the purity of the material. In an impure material the Cottrell atmosphere pins down the dislocations and so the recrystallisation begins at higher temperatures.

The behaviour of the $\nu_Q^{(1)}$ parameter value with increasing annealing temperature for samples of different degrees of deformation is shown in figure 3. In the temperature range 350–425 K a sharp decrease of $\nu_Q^{(1)}$ values was observed indicating the recovery stage. For more deformed samples this recovery stage starts at lower annealing temperatures. From the hyperfine interaction measurements alone, it cannot be decided whether the observed defects are pinned to impurities or not. The interaction of impurities with defects can alter the recovery of lattice damage which in some cases may be a serious drawback of the PAC technique. In the case of our measurements the absence of a well defined quadrupole frequency related to the trapping of dislocations at indium can suggest that In–dislocation interaction in silver is very weak. The comparison of observed recovery temperatures with the results of hardness [26, 35], residual resistivity [26, 30, 35] and positron lifetime experiments [36] in deformed silver is shown in figure 5, where the values of recovery stage V temperatures in silver are drawn as a function of the deformation degree. Our results are in good agreement with the general trend, although a little deviation in the direction of higher temperatures is observed which may be the consequence of insufficient purity of samples.

References

[1] Müller H G 1980 *Nuclear Physics Methods in Materials Research* ed. K Bethge, H Baumann, H Jax and F Rauch (Braunschweig: Vieweg) p 418
[2] Collins G S, Stern G P and Hohenemser C 1981 *Phys. Lett.* **84A** 289
[3] Müller H G 1982 *Z. Phys.* B **47** 119
[4] Deicher M, Grübel G and Reiner W 1987 *Mater. Sci. Forum* **15/18** 635
[5] Collins G S and Schuhmann R B 1983 *Hyperfine Interact.* **15/16** 391
[6] Collins G S, Allard C, Schuhmann R B and Hohenemser C 1985 *Phys. Rev.* B **32** 2940
[7] Petry W, Brüssler M, Gröger V, Müller H G and Vogl G 1983 *Hyperfine Interact.* **15/16** 371
[8] Collins G S 1987 *Mater. Sci. Forum* **15/18** 783
[9] Deicher M, Minde R and Wichert Th 1983 *Hyperfine Interact.* **15/16** 401
[10] Rinnberg H, Semmler W and Antesberger G 1978 *Phys. Lett.* **66A** 57
[11] Sassa K, Petry W and Vogl G 1983 *Phil. Mag.* A **48** 41
[12] Allard C, Collins G S and Hohenemser C 1985 *Phys. Rev.* B **32** 4839
[13] Arends A R, Hohenemser C, Pleiter F, de Waard H, Chow L and Suter R M 1980 *Hyperfine Interact.* **8** 191
[14] Diecher M, Recknagel E and Wichert Th 1981 *Hyperfine Interact.* **10** 675
[15] Thomé L and Bernas H 1976 *Phys. Rev. Lett.* **36** 1055
[16] Wodniecki P, Wodniecka B and Pham Quoc Hung 1981 *Acta Phys. Polon.* A **60** 817
[17] Echt O, Recknagel E, Weidinger A and Wichert Th 1978 *Z. Phys.* B **32** 59
[18] Deicher M, Recknagel E and Wichert Th 1981 *Radiat. Eff.* **54** 155
[19] Collins G S, Allard C, Reinhardt B, Schumann S and Hohenemser C 1983 *Phys. Rev.* B **28** 2940
[20] Pleiter F 1977 *Hyperfine Interact.* **5** 109
[21] Kanert O 1969 *Phys. Status Solidi* **32** 667
[22] Kanert O 1964 *Phys. Status Solidi* **7** 791
[23] Kanert O and Mehring M 1971 *NMR* vol 3, ed. P Diehl, E Fluck and R Kosfeld (Berlin: Springer) p 62
[24] Kanert O 1965 *Z. Phys.* **184** 92
[25] Bailey J E and Hirsch B 1960 *Phil. Mag.* **5** 485
[26] Clarebrough L M, Hargreaves M E and Loretto H 1962 *Phil. Mag.* **7** 115
[27] Swanson M L 1970 *Phys. Status Solidi* a **3** 287, 551
[28] Van den Beukel A 1970 *Vacancies and Interstitials in Metals* ed. A Seeger, D Schumacher, W Schilling and J Diehl (Amsterdam: North-Holland) p 247
[29] Tomizuka C T and Sonder E 1956 *Phys. Rev.* **103** 1182
[30] Ramsteiner F, Schüle W and Seeger A 1962 *Phys. Status Solidi* **2** 1005
[31] Kamel R and Attia E A 1961 *Acta Metall.* **9** 1047
[32] Semmel J W and Machlin E S 1957 *Acta Metall.* **5** 582
[33] Cuddy L J and Machlin E S 1962 *Phil. Mag.* **7** 745
[34] Doyama M and Koehler J S 1962 *Phys. Rev.* **127** 21
[35] Tamman G and Dreyer K L 1933 *Ann. Phys., Lpz.* **16** 111
[36] Wegner D 1988 *Preprint* II Phys. Inst. Univ. Göttingen